ARTICLE IN PRESS

Cytotherapy 000 (2022) 1-8



Contents lists available at ScienceDirect

CYTOTHERAPY

International Society

ISCT:

Cell & Gene Therapy®

journal homepage: www.isct-cytotherapy.org

Full-length article

Impact of storage conditions and duration on function of native and cargo-loaded mesenchymal stromal cell extracellular vesicles

Daniel Levy^{1,*}, Anjana Jeyaram^{1,*}, Louis J. Born¹, Kai-Hua Chang², Sanaz Nourmohammadi Abadchi², Angela Ting Wei Hsu², Talia Solomon¹, Amaya Aranda¹, Samantha Stewart¹, Xiaoming He¹, John W. Harmon², Steven M. Jay^{1,3,**}

ARTICLE INFO

Article History: Received 31 August 2022 Accepted 18 November 2022 Available online xxx

Key Words: exosomes HOTAIR microvesicles miR-146a-5p

ABSTRACT

Background aims: As evidenced by ongoing clinical trials and increased activity in the commercial sector, extracellular vesicle (EV)-based therapies have begun the transition from bench to bedside. As this progression continues, one critical aspect of EV clinical translation is understanding the effects of storage and transport conditions. Several studies have assessed the impact of storage on EV characteristics such as morphology, uptake and component content, but effects of storage duration and temperature on EV functional bioactivity and, especially, loaded cargo are rarely reported.

Methods: The authors assessed EV outcomes following storage at different temperatures (room temperature, 4° C, -20° C, -80° C) for various durations as well as after lyophilization.

Results: Mesenchymal stromal cell (MSC) EVs were observed to retain key aspects of their bioactivity (provascularization, anti-inflammation) for up to 4–6 weeks at –20°C and –80°C and after lyophilization. Furthermore, via *in vitro* assays and an *in vivo* wound healing model, these same storage conditions were also demonstrated to enable preservation of the functionality of loaded microRNA and long non-coding RNA cargo in MSC EVs

Conclusions: These findings extend the current understanding of how EV therapeutic potential is impacted by storage conditions and may inform best practices for handling and storing MSC EVs for both basic research and translational purposes.

© 2022 International Society for Cell & Gene Therapy. Published by Elsevier Inc. All rights reserved.

Introduction

Extracellular vesicles (EVs) are nanoscale cell-derived products that are considered promising therapeutic agents and drug delivery vehicles [1]. From a drug carrier perspective, EVs compare favorably to synthetic delivery systems with respect to cargo delivery efficiency, physiological transport properties and multi-functionality [2–5]. As native therapeutic agents, mesenchymal stromal cell (MSC) EVs, in particular, have been widely reported to be therapeutically useful in a variety of pre-clinical studies based on their anti-inflammatory and pro-angiogenic effects, leading to their use in clinical trials [6–8], yet several obstacles remain to be overcome prior to translation and widespread clinical application of MSC EV therapies.

Among these is a relative dearth of knowledge regarding the effects of storage conditions on MSC EV functionality.

As EVs lack much of the complex cellular machinery and organelles that exist in their parental cells, they may potentially be stored at more desirable conditions for clinical translation such as at -20°C or -80°C freezer storage at room temperature (RT) following lyophilization [9]. There have been some important initial studies in this area, specifically with regard to the morphological stability and enzymatic stability of EV cargos as well as determining appropriate buffers for EV storage [10-22]. Further, some knowledge about the effects of storage conditions on EV bioactivity has begun to accumulate. Wu et al. [23] recently demonstrated that cold storage of isolated bEnd.3 EVs at -20°C and -80°C for 28 days resulted in improved cellular uptake and in vivo circulation, whereas van de Wakker et al. [24] showed that cardiac progenitor cell-derived EVs retained their bioactivity in an endothelial cell gap closure assay after 7 days of storage at -80° C, with activity reduced over the same storage period at 4° C. However, despite these and other reports, much remains to be learned about how MSC EV function is impacted by storage.

¹ Fischell Department of Bioengineering, University of Maryland, College Park, Maryland, USA

² Department of Surgery, Johns Hopkins University School of Medicine, Baltimore, Maryland, USA

³ Program in Molecular and Cell Biology, University of Maryland, College Park, Maryland, USA

^{**} Correspondence: Steven M. Jay, PhD, Fischell Department of Bioengineering, University of Maryland, 8278 Paint Branch Dr, 3116 A. James Clark Hall, College Park, Maryland 20742, USA.

E-mail address: smjay@umd.edu (S.M. Jay).

^{*} These authors contributed equally to this work.

2

Here the authors add to the understanding of storage effects on EV activity with a focus on human bone marrow-derived MSC (BDMSC) EVs. Specifically, the authors' data showed that the anti-inflammatory and pro-angiogenic effects of MSC EVs were retained for up to 28 days after storage at -20°C, -80°C and RT following lyophilization. Furthermore, given the interest in EVs as drug delivery vehicles [25], the authors examined the effects of storage conditions on loaded microRNA (miRNA) cargo in MSC EVs, showing that although the total amount of cargo detected was decreased in all conditions tested, cargo-associated bioactivity was retained in several storage modes. Finally, the authors demonstrated that lyophilization was suitable for preservation of regenerative bioactivity of MSC EVs loaded with the long non-coding RNA HOTAIR in a db/db mouse wound healing model. Overall, these studies provide further guidance for the field on how EVs, and in particular drug-loaded MSC EVs, should be stored prior to therapeutic application.

Methods

Cell culture

Human BDMSCs (PC-500-012; American Type Culture Collection, Manassas, VA, USA) were cultured in Dulbecco's Modified Eagle's Medium (DMEM) [+] 4.5 g/L glucose, L-glutamine and sodium pyruvate supplemented with 10% EV-depleted fetal bovine serum (FBS), 1% penicillin-streptomycin and 1% non-essential amino acids in T-175 polystyrene tissue culture flasks. The 10% EV-depleted FBS was generated via centrifugation of FBS at $100\,000 \times g$ for 16 h before collection of the non-pelleted supernatant. BDMSCs were passaged at approximately 70% confluency until passage three or four before EV isolation for functional assays and passage five for EV characterization. Human umbilical vein endothelial cells (HUVECs) (C2519A; Lonza, Basel, Switzerland) were cultured in tissue culture flasks coated with 0.1% gelatin prior to seeding cells in endothelial growth medium (C-C22121; PromoCell, Heidelberg, Germany). RAW264.7 cells (TIB71; American Type Culture Collection) were cultured in DMEM [+] 4.5 g/L glucose, L-glutamine and sodium pyruvate supplemented with 1% penicillin-streptomycin and 5% FBS.

EV separation

BDMSCs were seeded in T-175 flasks at a density of 500 000 cells per flask and grown in EV-depleted medium for 2 days before the conditioned medium was collected and subjected to differential ultracentrifugation with a $100\,000 \times g$ final centrifugation step as previously described [26]. Pelleted EVs were resuspended in $1\times g$ phosphate-buffered saline (PBS) and subsequently washed using Nanosep 300-kDa molecular weight cutoff spin columns (OD300C35; Pall Corporation, Port Washington, NY, USA). Washed EVs were then resuspended in $1\times g$ PBS and sterilely filtered using a $0.2-\mu m$ syringe filter.

EV storage conditions

Post-isolation, EVs were resuspended in $1\times$ PBS, aliquoted and stored at RT, 4° C, -20° C or -80° C in polypropylene tubes. Separate aliquots were prepared for each storage time (1 week, 4 weeks, 6 weeks) and freeze—thaw cycle (one cycle, five cycles). Three replicate samples were prepared for each time point and storage condition. Isolated EVs were individually quantified via total protein amount, aliquoted and lyophilized using an SP VirTis AdVantage Pro Lyophilizer with Intellitronics Controller (SP Industries Inc, Warminster, PA, USA) and stored at RT for the designated storage time (1 week, 4 weeks, 6 weeks). Equal amounts of three replicate samples (normalized by protein content) were again prepared for each time point.

EV characterization

EVs were quantified by nanoparticle tracking analysis (NTA) using a NanoSight LM10 with NTA 2.3 analytical software (Malvern Panalytical Ltd, Malvern, UK). Isolated EVs were diluted to a concentration of approximately 10 μ g protein/mL and aliquoted for each of the indicated time and storage conditions before loading into the Nano-Sight analysis chamber at RT. Three samples were prepared for each time point. Each sample was analyzed in triplicate using three different fields of view with a 60-s video acquisition time. The camera level and threshold were set at 16 and 7, respectively, for all samples.

Total EV protein amount was determined via bicinchoninic acid (BCA) assay following the manufacturer's protocol (ThermoFisher Scientific, USA). Protein levels were determined with three replicate samples for each time point, and each sample was measured in duplicate. Based on the day 0 protein amount, samples containing 20 μ g of protein were aliquoted for each time point for total protein quantification and western blots. At each time point, samples were prepared and stored until the blot was run. Total protein stains were done using a Swift membrane stain (G-Biosciences, St Louis, MO, USA). The membrane was imaged using an Odyssey CLx imager (LI-COR, Inc, Lincoln, NE, USA). Specific EV protein marker levels were quantified using western blot analysis for ALIX (ab186429; Abcam, Cambridge, UK) at 1:1000, TSG101 (ab125011; Abcam) at 1:1000, calnexin (2679S, C5C9; Cell Signaling Technology, Inc, Danvers, MA, USA) at 1:1000, flotillin-1 (ab133497; Abcam) at 1:1000, CD63 (Y402575; Applied Biological Materials (https://www.abmgood.com/anti-cd63antibody-y402575.html#Y402575)) at 1:200 and glyceraldehyde 3phosphate dehydrogenase (D16H11, 5174; Cell Signaling, Technology, Inc) at 1:2000 incubated over two nights at 4°C while shaking. Goat anti-rabbit IRDye 800CW (925-32210; LI-COR, Inc) secondary antibody was used at a 1:10000 dilution. Bands were detected with an Odyssey CLx imager and quantified using Image Studio (LI-COR, Inc).

To obtain transmission electron microscopy images, a negative staining technique was utilized. Isolated EVs were briefly incubated with an aqueous solution of electron microscopy-grade paraformal-dehyde (157-4-100; Electron Microscopy Sciences, Hatfield, PA, USA) before a carbon film grid (CF200-Cu-25; Electron Microscopy Sciences) was floated on a droplet of the mixture to incubate. The carbon grid was then washed before being floated on a droplet of 1% glutar-aldehyde. The grid was again washed before flotation on a droplet of uranyl acetate replacement stain (22405; Electron Microscopy Sciences). Prepared electron microscopy grids were then stored before imaging on a JEM 2100 LaB6 transmission electron microscope (JEOL USA, Inc, Peabody, MA, USA).

In vitro bioactivity assays

To assess endothelial gap closure, HUVECs (passage five) were seeded in 48-well plates in endothelial growth medium and allowed to grow until the formation of a confluent monolayer. The cell monolayer was then disrupted using a pipette tip to form a scratch. After washing, the cells were serum-starved for 2 h, after which the medium was replaced with the treatments. Endothelial growth medium and endothelial basal medium were used as positive and negative controls, respectively. Experiments with day 0 BDMSC EVs were conducted on the day of isolation, and the remaining EVs were stored at the indicated conditions or freeze—thaw cycles. After storage, another gap closure assay was performed with the samples at those time points. The gap area was imaged at both 0 h and 11 h. The change in denuded area was quantified using ImageJ.

Endothelial tube formation was assessed using HUVECs (passage five). Cells were washed, trypsinized and diluted in endothelial basal medium supplemented with 0.1% FBS before cell counting. HUVECs were then aliquoted and pelleted at 300 \times g, at which point the

supernatant was removed and the cells were resuspended in their respective treatments of stored BDMSC EVs ($100~\mu g/mL$) in endothelial basal medium. Resuspended HUVECs were then added to 24-well plates coated with growth factor-reduced Matrigel (356252; Corning, Corning, NY, USA) at a seeding density of $75\,000$ cells/well. Phase-contrast images of tube-forming HUVECs were then taken after 2-12 h, and the number of branch points was quantified using Image].

To evaluate the effects of EVs on IL-6 secretion, RAW264.7 mouse macrophages were seeded into 48-well plates in DMEM supplemented with 5% FBS and 1% penicillin-streptomycin at a density of 100 000 cells/well. At 24 h post-seeding, RAW264.7 macrophages were pre-treated with no treatment, dexamethasone (D4902-25MG; Sigma-Aldrich, St Louis, MO, USA) or the given BDMSC EV treatment (100 μ g/mL) in cell culture medium. A total of 24 h later, RAW264.7 treatments were removed and replaced with 10 ng/mL lipopolysaccharide (LPS) (L4391-1MG; Sigma-Aldrich) in DMEM supplemented with 5% FBS and 1% penicillin-streptomycin for an additional 4 h. After LPS treatment, cell supernatants were collected and stored at -80°C before assessment via enzyme-linked immunosorbent assay. IL-6 levels from RAW264.7-conditioned medium were quantified using a DuoSet enzyme-linked immunosorbent assay kit (DY406; R&D Systems, Inc, Minneapolis, MN, USA) following the manufacturer's instructions.

EV loading via sonication

The same day as BDMSC EV isolation, EVs were loaded with an miR-146a-5p mimic (C-300630-03-0050; Dharmacon, Lafayette, CO, USA) as previously described [27]. Next, 100 μg of EVs was incubated with 1000 pmol of miR-146a-5p in 100 μL of PBS for 30 min. EVs were then sonicated twice in a Symphony water bath sonicator (97043-964; VWR International, LLC, Radnor, PA, USA) with a 2.8-L capacity (24 \times 14 \times 10 cm) for 30 s at 35 Hz, resting on ice for 1 min between sonications. After sonication, EVs were washed three times in a 300-kDa molecular weight cutoff filter with 1 \times PBS. Loaded EVs were then pooled, quantified for total protein content via BCA assay and aliquoted for storage in their respective conditions.

At the indicated time points and storage conditions, loaded BDMSC EV samples were placed in 700 μ L QIAzol lysis reagent (79306; QIAGEN, Hilden, Germany) spiked with 2 fmol cel-miR-39 (59000; Norgen Biotek Corp, Thorold, Canada) as an internal control. Total RNA was isolated with an miRNeasy mini kit (217004; QIAGEN) following the manufacturer's instructions. Post-RNA isolation, complementary DNA was generated from isolated total RNA samples using an miScript II reverse transcription kit (218161; QIAGEN). Complementary DNA was stored at -20°C before quantitative polymerase chain reaction (qPCR), which was performed on a QuantStudio 7 Flex gPCR system (4485701; Thermo Fisher Scientific, Waltham, MA, USA) using SsoAdvanced Universal SYBR (1725271; Bio-Rad Laboratories, Inc, Hercules, CA, USA). Transcripts for miR-146a-5p were quantified with cel-miR-39 as the internal control. The polymerase chain reaction primer sequences were as follows: miR-146a-5p forward, CGCAGGAGAACTGAATTCCA; miR-146a-5p reverse, CAGTTTTTTTTTTTT; cel-miR-39 forward, GTCACCGGGTGATAAAT-CAG; and cel-miR-39 reverse, GGTCCAGTTTTTTTTTTTTTCAAG. Transcript expression was calculated using the comparative Ct method normalized to cel-miR-39 (2- $\Delta\Delta$ Ct) and expressed as fold change of miR-146a-5p transcripts in storage groups versus freshly loaded EVs.

Animal studies

Passage four BDMSCs were seeded at 500 000 cells per T-175 flask before transfection with a pCMV-HOTAIR plasmid as previously described [26]. Specifically, pCMV-HOTAIR was transfected into BDMSCs via Lipofectamine 3000 (L30000015; Thermo Fisher

Scientific) for 1 h before washing and then growing in EV-depleted medium. Conditioned medium was then collected on day 3 to day 6 post-transfection and isolated via ultracentrifugation as described earlier before subsequent lyophilization. Next, db/db mice (The Jackson Laboratory, Bar Harbor, ME, USA) weighing 40–50 g were anesthetized with isoflurane, and the dorsum of each mouse was then shaved. An 8-mm punch biopsy was taken from the shaved region of each mouse, and buprenorphine (0.05 mg/kg) was subcutaneously injected on day 0, day 1 and day 3. On day 3, four subcutaneous injections (1 μ g/ μ L, 50 μ L) were given to each mouse in a cross pattern. Eight mice were used for each treatment group. Wound tracing and wound closure were determined as previously described [26]. All animal experiments were performed in compliance with the National Institutes of Health Guide for the Care and Use of Laboratory Animals.

Statistical analysis

Two-way analysis of variance with Dunnett multiple comparison test (compared with day 0 measurements) was utilized to determine statistical significance in all *in vitro* experiments. Two-way analysis of variance with Holm—Šídák multiple comparison test was used to determine statistical significance in *in vivo* wound healing time course experiments. Statistical analyses were performed with Prism 9 (GraphPad Software, Inc, San Diego, CA, USA).

Results

Frozen storage and lyophilization lead to increased EV size with little change in EV-associated proteins

EVs were isolated from the conditioned medium of BDMSCs via ultracentrifugation and then aliquoted and stored in each of their respective conditions and time points. EV size distribution and concentration were assessed for each storage condition via NTA using a NanoSight LM10. Size distributions of isolated EVs were within expected size ranges, with a representative distribution of BDMSC EVs demonstrated (approximately 128-nm mode size) (Figure 1A). In the authors' storage studies, an increase in mode size (113-143 nm) was observed after 28 days of storage at -20°C (Figure 1B). After five freeze-thaw cycles at -80°C, the authors observed a non-statistically significant increase in mode size (113-145 nm) (Figure 1C). The increase in size was postulated to be due to aggregation of EVs during storage, which was supported by an observed increase in mean size, as detected via NTA (see supplementary Figure 1). Transmission electron microscopy analysis also confirmed that EV morphology was retained after lyophilization (Figure 1D). Further, the authors did not observe significant changes to EV protein markers CD63 and TSG101 with storage at RT, 4°C, -20°C and -80°C or after up to five freeze-thaw cycles, as determined by immunoblotting (Figure 1E).

Again, isolated BDMSC EVs were aliquoted and stored in their respective conditions and time points before assessing total protein content using a BCA assay. Although storage at -20°C and -80°C generally preserved total protein content, the authors observed a slight trend of decreasing protein content over up to 28 days when stored at RT and 4°C (Figure 1F). Furthermore, when subjected to freeze—thaw cycles, a non-statistically significant decrease in total protein concentration was observed after five freeze—thaw cycles at both -20°C and -80°C (Figure 1G). Total protein content within separate isolated BDMSC EV samples was determined via BCA assay, and aliquots equivalent to $100~\mu\text{g}$ were lyophilized and stored for either 7 days or 28 days before reassessing total protein content. The authors observed that lyophilization largely preserved the total protein content of BDMSC EVs (Figure 1H).



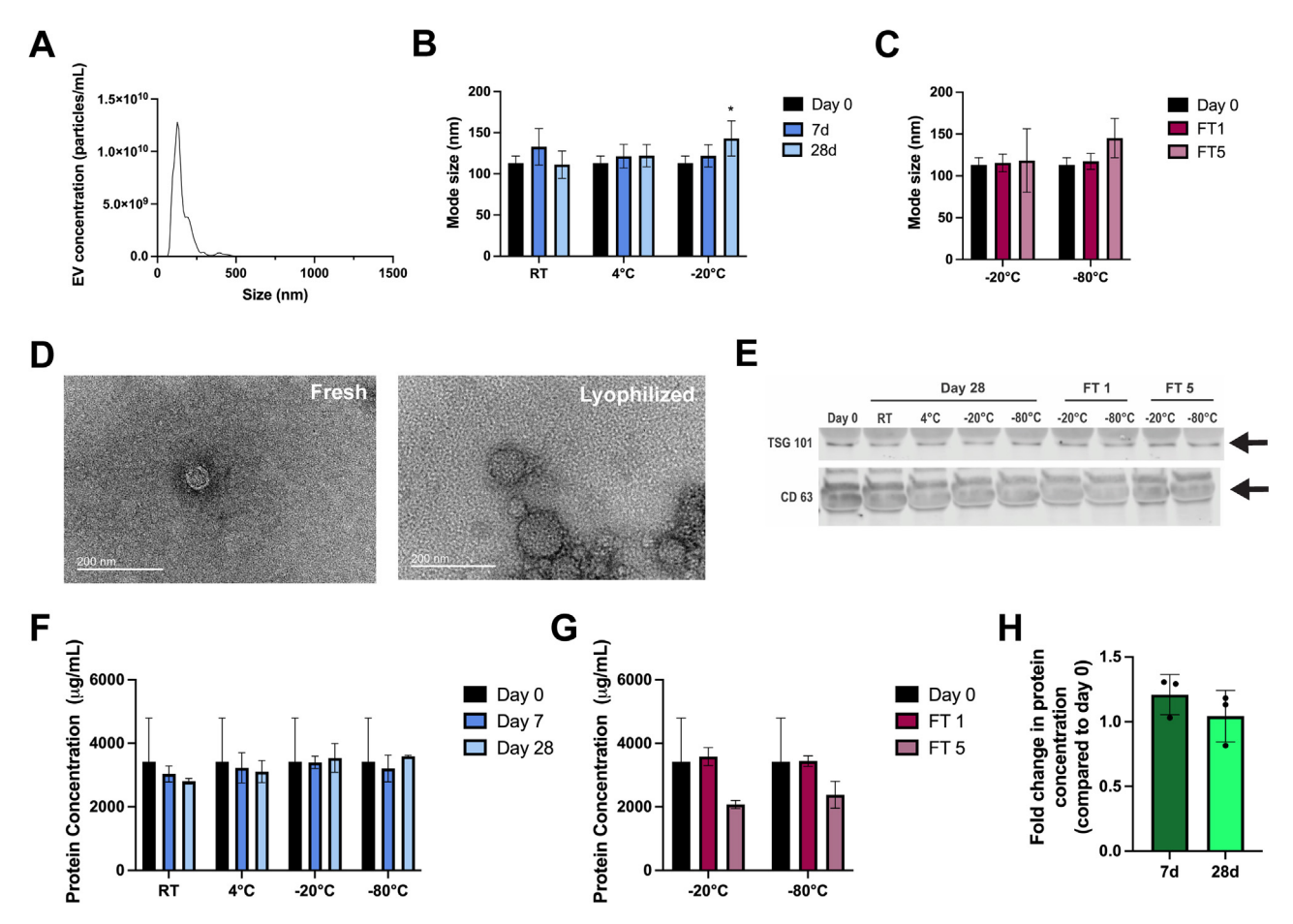


Fig. 1. Morphological, size and protein characterization of stored BDMSC EVs. (A) Representative concentration and size distribution profile of isolated BDMSC EVs as assessed by NTA. (B) Mode size (diameter) changes under various BDMSC EV storage conditions at day 0, day 7 and day 28. (C) Mode size (diameter) changes in BDMSC EVs after FT1 and FT5 compared with day 0. (D) TEM images of isolated BDMSC EVs immediately after isolation or lyophilization and reconstitution. (E) Immunoblot analysis of BDMSC EV markers TSG101 and CD63 after storage at RT, 4° C, -20° C or -80° C or FT1 and FT5. (F) BDMSC EV protein concentration at RT, 4° C, -20° C or -80° C after 7 days or 28 days compared with day 0. Concentration determined via BCA assay. (G) BDMSC EV protein concentration after FT1 or FT5 compared with day 0 as assessed via BCA assay. (H) Changes in BDMSC EV protein concentration following lyophilization and storage at RT for 7 days or 28 days compared with pre-lyophilization. Data are representative of three independent experiments. All values are expressed as mean \pm standard deviation. $^{\circ}$ P < 0.01. FT, freeze—thaw; TEM, transmission electron microscopy.

Preservation of BDMSC EV in vitro bioactivity is greatly impacted by storage conditions

EVs were isolated from BDMSC-conditioned medium via ultracentrifugation and then aliquoted and stored for 4 weeks at RT, 4°C, -20°C, -80°C or RT after lyophilization. Vascularization bioactivity of stored BDMSC EVs was then assessed via an endothelial gap closure assay, with freshly isolated BDMSC EVs from the same donor used as a positive control. At a dose of 100 μ g/mL, the freshly isolated, -20° C, -80°C and lyophilized BDMSC EV groups induced an increase in HUVEC gap closure compared with the negative control, whereas the RT and 4°C treatment groups resulted in no observable improvement compared with the negative control medium condition (Figure 2A). To test whether freeze-thaw cycles had an impact on BDMSC EV bioactivity, EVs were isolated and stored at either -20°C or -80°C and subjected to either one or five freeze-thaw cycles while in storage for 7 days. In another gap closure assay, the authors observed that although one freeze-thaw cycle had minimal impact on gap closure, five cycles led to a marginal decrease in gap closure compared with freshly isolated BDMSC EVs (Figure 2B).

To confirm whether the *in vitro* pro-vascularization potential of BDMSC EVs was impacted by storage conditions, a similar treatment scheme was performed using an endothelial tube formation assay. A significant decrease in bioactivity of BDMSC EVs stored at RT was observed, whereas -20°C , -80°C and lyophilization preserved bioactivity (Figure 2C). Interestingly, storage at 4°C also

preserved the ability of BDMSC EVs to induce tube formation. The tube formation assay was also performed using the freeze—thaw groups at -20° C and -80° C and one or five freeze—thaw cycles. As in the gap closure assay, one freeze—thaw cycle had no effect on bioactivity, whereas a slight decrease was observed after five cycles at -80° C (Figure 2D).

To further confirm whether key BDMSC EV bioactivities were impacted by storage conditions, the anti-inflammatory effects of BDMSC EVs were assessed in an LPS-stimulated RAW264.7 mouse macrophage model, with the key output being the amount of proinflammatory IL-6 secreted post-LPS stimulation, as this has been shown to correlate with MSC EV anti-inflammatory activity in vivo [28]. Using 6-week storage time as an endpoint, the authors observed that BDMSC EVs from the RT and 4°C groups lost their ability to attenuate IL-6 secretion compared with freshly isolated BDMSC EVs (Figure 2E). BDMSC EVs stored at -20°C and -80°C lowered IL-6 secretion but to a lesser extent than freshly isolated EVs. Additional experiments revealed that BDMSC anti-inflammatory activity, as measured by this assay, was reduced after 4 weeks of storage at 4°C, with continued loss of activity over time, whereas activity was retained in EVs stored at -20° C and -80° C for up to 8 weeks (see supplementary Figure 2). Interestingly, lyophilized BDMSC EVs stored at RT completely preserved the ability to reduce IL-6 levels. It was confirmed in the LPS-stimulated RAW264.7 mouse macrophage model that the impact of freeze-thaw cycles on BDMSC EV bioactivity was negligible over the course of 1 week (Figure 2F).

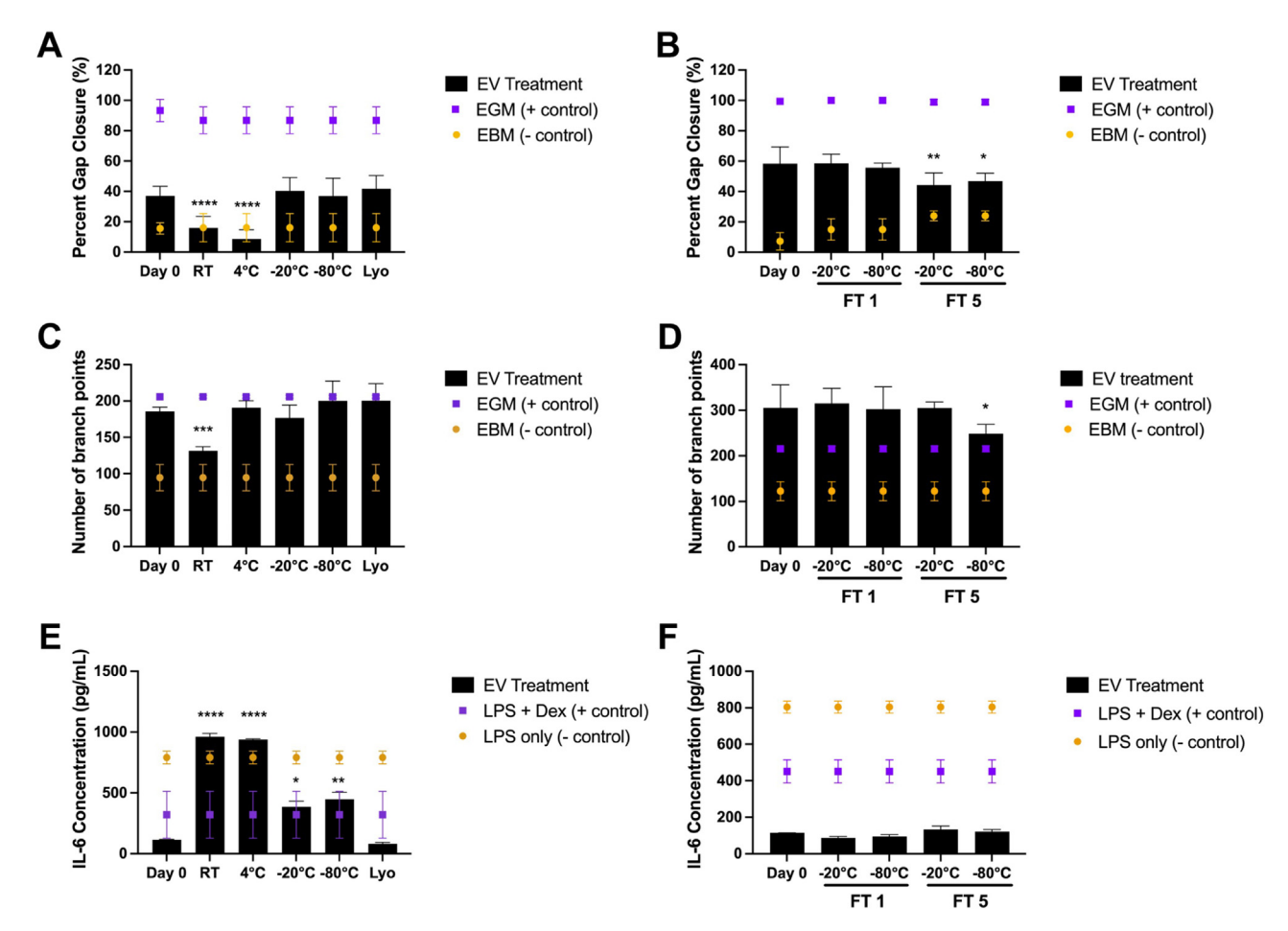


Fig. 2. Storage conditions affect EV therapeutic functionality *in vitro*. (A) Post-scratch induction, HUVECs were treated with EGM (positive control), EBM (negative control) or 100 μ g/mL BDMSC EVs stored for 4 weeks at RT, 4°C, -20°C or -80°C or Lyo (stored at RT after lyophilization). Changes in gap closure were compared with BDMSC EVs isolated at day 0, before storage. (B) Post-scratch induction, HUVECs were treated with EGM, EBM or 100 μ g/mL BDMSC EVs after storage at -20°C or -80°C and FT1 or FT5. Changes in gap closure were compared with BDMSC EVs isolated at day 0, before storage and FT. (C) Tube formation capabilities of HUVECs after treatment with BDMSC EVs stored at RT, 4°C, -20°C or -80°C or Lyo for 4 weeks. (D) Tube formation capabilities of HUVECs after treatment with BDMSC EVs after storage at -20°C or -80°C and FT1 or FT5. (E) RAW264.7 macrophages were pre-treated with BDMSC EVs stored at RT, 4°C, -20°C or -80°C or Lyo (6-week storage time). RAW264.7 macrophages were treated with LPS before cell supernatans were collected, and IL-6 levels were quantified via ELISA. (F) RAW264.7 macrophages were pre-treated with BDMSC EVs stored at -20°C or -80°C and FT1 or FT5. Similarly, after LPS stimulation, IL-6 levels in cell supernatants were quantified via ELISA. All values are expressed as mean \pm standard deviation. * $^{*}P < 0.05$, * $^{*}P < 0.001$, * $^{**}P < 0.001$, * $^{**}P < 0.0001$. Dex, dexamethasone; EBM, endothelial basal medium; EGM, endothelial growth medium; ELISA, enzyme-linked immunosorbent assay; FT, freeze—thaw; Lyo, lyophilized.

Storage of miRNA-loaded EVs at -20° C and -80° C and after lyophilization better preserves miRNA content and bioactivity compared with higher-temperature storage conditions

A significant aspect of the therapeutic potential associated with EVs lies in their use as drug carriers. To assess the effects of storage conditions on cargo-loaded EVs, a sonication method previously validated by the authors' group was chosen for loading of miRNA, which is of particular interest with respect to EV-mediated delivery [27]. BDMSC EVs were again isolated using ultracentrifugation before subsequent total protein quantification via BCA assay. Isolated EVs were then promptly co-incubated and sonicated with miR-146a-5p (previously identified as having anti-inflammatory effects) at a ratio of 100 μg EVs to 1000 pmol miR-146a-5p as previously described [29]. miR-146a-5p-loaded BDMSC EVs were then assessed by NTA (see supplementary Figure 4) and quantified via BCA assay and aliquoted and stored at RT, 4°C, -20°C or -80°C or lyophilized and stored at RT for 4 weeks. After 4 weeks, miR-146a-5p-loaded BDMSC EV samples at each storage condition were again aliquoted and subjected to RNA isolation, reverse transcription and qPCR or the previously described mouse macrophage inflammatory model. Before RNA isolation and subsequent qPCR, 2 fmol of celmiR-39 was spiked in as an internal control for the RNA isolation and reverse transcription steps. qPCR results demonstrated that, compared with freshly loaded EVs, loaded EVs stored at RT, 4°C, -20°C or -80°C or lyophilized and stored at RT had marked decreases in miR-146a-5p levels of approximately 99.7%, 95.3%, 80.5%, 81.4% and 75.1%, respectively (Figure 3A).

Interestingly, when utilized in the RAW264.7 mouse macrophage inflammatory model at a dose of 40 $\mu g/mL$ post-sonication, miR-146a-5p-loaded BDMSC EVs reduced IL-6 levels at a higher rate than unloaded BDMSC EVs in general. However, changes based on storage conditions were less pronounced, with only loaded EVs stored at RT leading to significantly reduced anti-inflammatory capabilities (Figure 3B). The authors also observed that miR-146a-5p-loaded BDMSC EVs stored at $-80^{\circ}\mathrm{C}$ reduced IL-6 levels more than freshly loaded BDMSC EVs, although this outcome may be explained by slight variations within the RAW264.7 assay itself or during the sonication process.

BDMSC EVs loaded with miR-146a-5p were stored at -20°C and -80°C and subsequently subjected to one or five freeze—thaw cycles. Analysis of these samples yielded highly variable miR-146a-5p levels, as assessed by qPCR (Figure 3C). However, in the stimulated RAW264.7 mouse macrophage assay, no statistical differences between miR-146a-5p-loaded BDMSC EVs subjected to freeze—thaw cycles and freshly loaded EVs were observed (Figure 3D).

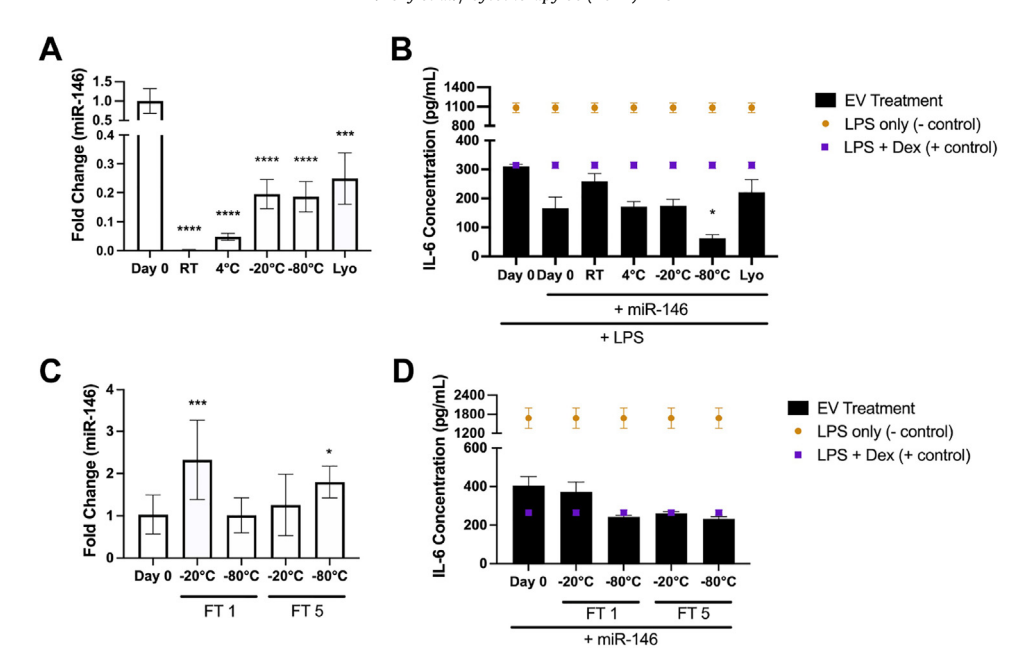


Fig. 3. Effects of storage conditions on miRNA content and bioactivity of loaded EVs. (A) Levels of miR-146a-5p in sonicated BDMSC EVs were quantified via qPCR after storage at RT, 4° C, -20° C or -80° C or Lyo (4-week storage time). Fold change of miR-146a-5p was compared with day 0 isolated/loaded BDMSC EVs, with 2 fmol cel-miR-39 spiked into samples before RNA isolation as an internal control. Non-sonicated BDMSC EVs were used as a loading control. (B) RAW264.7 macrophages were pre-treated with miR-146a-5p-loaded BDMSC EVs stored at 4° C, -20° C or -80° C or Lyo (4-week storage time). RAW264.7 macrophages were treated with LPS before cell supernatants were collected, and IL-6 levels were quantified via ELISA. (C) Levels of miR-146a-5p in sonicated BDMSC EVs were quantified via qPCR after storage at -20° C or -80° C and FT1 or FT5 over 1 week. cel-miR-39 spiked into samples was again used as an internal control, and miR-146a-5p levels were compared with day 0 isolated/loaded BDMSC EVs. Non-sonicated BDMSC EVs were again used as a loading control. (D) RAW264.7 macrophages were pre-treated with miR-146a-5p-loaded BDMSC EVs stored at -20° C or -80° C and FT1 or FT5. Similarly, after LPS stimulation, IL-6 levels in cell supernatants were quantified via ELISA. All values are expressed as mean \pm standard deviation. $^{\circ}P < 0.05$, $^{****}P < 0.001$, $^{****}P < 0.0001$. Dex, dexamethasone; ELISA, enzyme-linked immunosorbent assay; FT, freeze—thaw; Lyo, lyophilized.

Lyophilization preserves wound healing bioactivity of enhanced BDMSC EVs in vivo

As lyophilization adequately preserved the pro-angiogenic and anti-inflammatory capabilities of BDMSC EVs *in vitro*, the authors assessed whether these effects translated to a clinically relevant animal model. Previously, the authors demonstrated that BDMSC EVs loaded with the long non-coding RNA HOTAIR enhanced wound closure after an 8-mm punch biopsy on the dorsum of db/db mice, whereas unaltered BDMSC EVs did not [26]. Thus, the authors lyophilized HOTAIR-loaded BDMSC EVs and stored them at RT for 4 weeks before reconstituting and using them in the same db/db mouse model. The authors observed that, compared with the PBS vehicle control, lyophilized HOTAIR-loaded BDMSC EVs improved wound healing at a rate comparable to that of fresh HOTAIR-loaded BDMSC EVs (wound closure of 81 \pm 10%, 90 \pm 8.5% and 92.8 \pm 7%, respectively) (Figure 4).

Discussion

EV-based therapies are drawing increasing interest for therapeutic translation for a wide variety of applications [30,31]. However, to fully realize the clinical potential of EVs, it is vital to increase understanding and optimization of manufacturing parameters such as storage conditions. This reality was reinforced during the rollout of coronavirus disease 2019 vaccines, with required storage conditions greatly affecting which populations are able to access a given therapeutic [32]. Here the authors aimed to determine appropriate storage conditions for MSC EVs, finding that bioactivity of both native and cargo-loaded MSC EVs was affected by storage temperature especially. The data also reinforce the concept that lyophilization can be employed successfully for EV storage. These findings have implications for basic EV research and eventual clinical translation of EV therapeutics.

Several of the authors' findings are supported by prior work in the field. For example, the authors' results suggest that storage of EVs at -20°C and increased freeze—thaw cycles lead to EV aggregates, as evidenced by an observed increase in size via NTA (Figure 1B,C). This finding is reinforced by Wu *et al.* [23], in which a decrease in both total protein content and total RNA content was observed at higher storage temperatures (RT, 4°C) as well as after multiple freeze—thaw cycles. Additionally, the authors' data show that pro-vascularization and anti-inflammatory bioactivity of BDMSC EVs is diminished after storage at RT and 4°C, whereas storage at -20°C or -80°C or lyophilization generally preserves bioactivity to a greater degree for up to 4 weeks (Figure 2). This expands on the study by van de Wakker *et al.* [24], which showed that cardiac progenitor cell-derived EVs exhibited bioactivity in an endothelial cell gap closure assay after 7 days of storage at -80°C but not 4°C .

This work additionally breaks new ground in reporting the effects of storage conditions on cargo-loaded MSC EVs. Using a previously described sonication approach [27] to load BDMSC EVs with the antiinflammatory miR-146a-5p, the authors observed that cargo-associated enhanced anti-inflammatory effects were retained in several storage conditions despite an apparent decrease in cargo levels (Figure 3). This could indicate that miR-146a-5p-loaded BDMSC EVs require relatively few copies per EV to achieve profound anti-inflammatory effects, which fits with prior observations that EVs deliver RNA cargo to cells in a highly efficient manner compared with synthetic delivery systems [2]. There results may additionally suggest that miRNAs that are not tightly bound to or associated with EVs are responsible for the majority of the observed miRNA signal in the control group, and that these miRNAs are removed during the additional washing steps associated with various storage conditions. In this case, additional preparation steps using detergents, enzymes or other methods to degrade miRNAs interacting with EV membranes may be useful for determining more accurate cargo loading levels for predicting bioactivity in future studies.

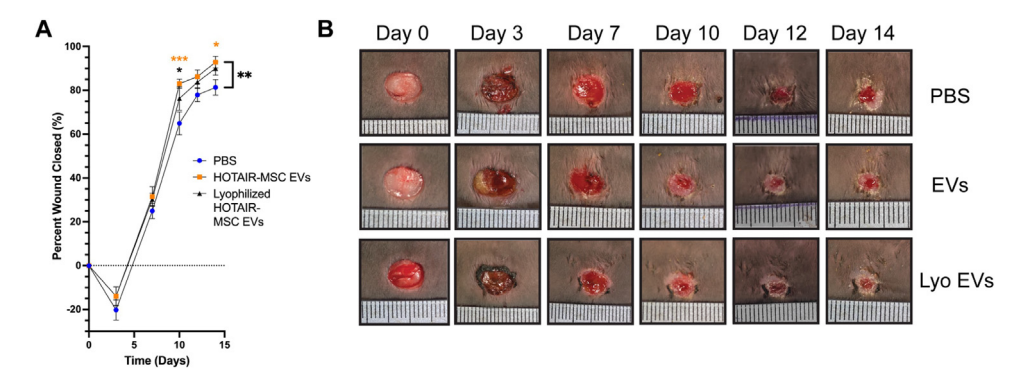


Fig. 4. Lyophilization preserves bioactivity of HOTAIR-loaded MSC EVs. Lyophilization and storage at RT for 4 weeks preserved the ability of HOTAIR-loaded BDMSC EVs to accelerate healing in a db/db mouse wound healing model over the course of 2 weeks. (A) Quantification of wound closure as determined by digital planimetry. (B) Images of wounds at indicated time points. All values are expressed as mean \pm standard deviation. *P < 0.05, **P < 0.01, ***P < 0.001. Lyo, lyophilized.

Critically, the authors observed that lyophilization of HOTAIR-loaded BDMSC EVs preserved their enhanced bioactivity in a db/db wound healing mouse model (Figure 4), indicating that lyophilization and storage at RT are suitable for retaining the activity of enhanced EVs. This is a vast improvement compared with cell-based therapies that require liquid nitrogen phase storage during transport and upon receipt in the clinic, further supporting the translatability of EV therapeutics [33].

There are several limitations to the present study that are worth mentioning. The authors' experiments were limited in duration and did not necessarily account for the full time span of stability and functionality that would be expected of a clinical EV product. Additional studies over longer periods of time are warranted. Further, there are additional considerations for fully determining optimal EV preservation conditions beyond what was studied here. Specifically, studies investigating optimal freezing buffers, vessels and the use of cryoprotectants to reduce the formation of ice crystals have been performed previously [11,15,34-36]. Together with the present work, these studies provide a foundation for determining the optimal storage conditions of MSC EVs for preservation of morphology and functionality. Given the current knowledge in the field and based on the present data, the authors recommend that isolated BDMSC EVs be stored at either -20° C or -80° C or lyophilized for up to 4 weeks while minimizing the number of freeze-thaw cycles before in vitro functional bioactivity studies or in vivo pre-clinical use.

Conclusions

Overall, the authors' data suggest that both storage conditions and duration may have a consequential effect on the therapeutic efficacy of bioactive MSC EVs—including those loaded with therapeutic cargo—in both basic research and clinical translation, with storage at -20°C and -80°C and lyophilization providing adequate retention of EV activity.

Funding

This work was supported by the National Institutes of Health (SMJ; HL141611, NS110637, GM130923, HL141922) and the National Science Foundation (SMJ; 1750542). DL and LJB were supported by A. James Clark Doctoral Fellowships from the University of Maryland. JWH was supported by the National Institutes of Health (HL141611) and the Hendrix Burn/Wound Fund of Johns Hopkins University. XH was supported by the National Science Foundation (CBET-18131019). SS was supported by the National Science Foundation Graduate Research Fellowship Program (grant no. DGE 1840340).

Author Contributions

Conception and design of the study: DL, AJ, XH, JWH, SMJ. Acquisition of data: DL, AJ, LJB, KC, SNA, ATWH, TS, AA, SS. Analysis and interpretation of data: DL, AJ, LJB, JWH, SMJ. Drafting or revising the manuscript: DL, AJ, SMJ.

Declaration of Competing Interest

The authors have no commercial, proprietary or financial interest in the products or companies described in this article.

Supplementary materials

Supplementary material associated with this article can be found in the online version at doi:10.1016/j.jcyt.2022.11.006.

References

- [1] Murphy DE, de Jong OG, Brouwer M, Wood MJ, Lavieu G, Schiffelers RM, et al. Extracellular vesicle-based therapeutics: natural versus engineered targeting and trafficking. Exp Mol Med. 2019;51(3):1–12.
- [2] Murphy DE, de Jong OG, Evers MJW, Nurazizah M, Schiffelers RM, Vader P. Natural or synthetic RNA delivery: a stoichiometric comparison of extracellular vesicles and synthetic nanoparticles. Nano Lett 2021;21(4):1888–95.
- [3] Lenzini S, Bargi R, Chung G, Shin J-W. Matrix mechanics and water permeation regulate extracellular vesicle transport. Nat Nanotechnol. 2020;15(3):217–23.
- [4] Osorio-Querejeta I, Carregal-Romero S, Ayerdi-Izquierdo A, Mäger I, L A N, Wood M, et al. Mik-219a-5p enriched extracellular vesicles induce OPC differentiation and EAE improvement more efficiently than liposomes and polymeric nanoparticles. Pharmaceutics 2020;12(2):186.
- [5] Witwer KW, Wolfram J. Extracellular vesicles versus synthetic nanoparticles for drug delivery. Nat Rev Mater 2021;6(2):103–6.
- [6] Kordelas L, Rebmann V, Ludwig A-K, Radtke S, Ruesing J, Doeppner TR, Epple M, Horn PA, Beelen DW, Giebel B. MSC-derived exosomes: a novel tool to treat therapy-refractory graft-versus-host disease. Leukemia 2014;28(4):970–3.
- [7] Nassar W, El-Ansary M, Sabry D, Mostafa MA, Fayad T, Kotb E, et al. Umbilical cord mesenchymal stem cells derived extracellular vesicles can safely ameliorate the progression of chronic kidney diseases. Biomater Res. 2016;20:21.
- [8] Ren S, Chen J, Duscher D, Liu Y, Guo G, Kang Y, et al. Microvesicles from human adipose stem cells promote wound healing by optimizing cellular functions via AKT and ERK signaling pathways. Stem Cell Res Ther. 2019;10(1):47.
- [9] Elsharkasy OM, Nordin JZ, Hagey DW, de Jong OG, Schiffelers RM, El Andaloussi S, et al. Extracellular vesicles as drug delivery systems: why and how? Adv Drug Deliv Rev. 2020;159:332–43.
- [10] Schulz E, Karagianni A, Koch M, Fuhrmann G. Hot EVs—how temperature affects extracellular vesicles. Eur J Pharm Biopharm Off J Arbeitsgemeinschaft Pharm Verfahrenstechnik EV 2020;146:55–63.
- [11] Charoenviriyakul C, Takahashi Y, Nishikawa M, Takakura Y. Preservation of exosomes at room temperature using lyophilization. Int J Pharm 2018;553(1–2):
- [12] Noguchi K, Hirano M, Hashimoto T, Yuba E, Takatani-Nakase T, Nakase I. Effects of Lyophilization of Arginine-rich Cell-penetrating Peptide-modified Extracellular Vesicles on Intracellular Delivery. Anticancer Res 2019;39(12):6701–9.

- [13] Cheng Y, Zeng Q, Han Q, Xia W. Effect of pH, temperature and freezing-thawing on quantity changes and cellular uptake of exosomes. Protein Cell 2019;10 (4):295–9
- [14] Deville S, Berckmans P, Hoof RV, Lambrichts I, Salvati A, Nelissen I. Comparison of extracellular vesicle isolation and storage methods using high-sensitivity flow cytometry. PLoS One 2021;16(2):e0245835.
- [15] Lőrincz ÁM, Timár CI, Marosvári KA, Veres DS, Otrokocsi L, Kittel Á, et al. Effect of storage on physical and functional properties of extracellular vesicles derived from neutrophilic granulocytes. J Extracell Vesicles 2014;3:25465.
- [16] Maroto R, Zhao Y, Jamaluddin M, Popov VL, Wang H, Kalubowilage M, et al. Effects of storage temperature on airway exosome integrity for diagnostic and functional analyses. J Extracell Vesicles 2017;6(1):1359478.
- [17] Jin Y, Chen K, Wang Z, Wang Y, Liu J, Lin L, Shao Y, Gao L, Yin H, Cui C, Tan Z, Liu L, Zhao C, Zhang G, Jia R, Du L, Chen Y, Liu R, Xu J, Hu X, Wang Y. DNA in serum extracellular vesicles is stable under different storage conditions. BMC Cancer 2016:16:753.
- [18] Ge Q, Zhou Y, Lu J, Bai Y, Xie X, Lu Z. miRNA in Plasma Exosome is Stable under Different Storage Conditions. Molecules 2014;19(2):1568–75.
- [19] Tegegn TZ, De Paoli SH, Orecna M, Elhelu OK, Woodle SA, Tarandovskiy ID, et al. Characterization of procoagulant extracellular vesicles and platelet membrane disintegration in DMSO-cryopreserved platelets. J Extracell Vesicles 2016:5:30422.
- [20] Zhou H, Yuen PST, Pisitkun T, Gonzales PA, Yasuda H, Dear JW, Gross P, Knepper MA, Star RA. Collection, storage, preservation, and normalization of human urinary exosomes for biomarker discovery. Kidney Int 2006;69(8):1471–6.
- [21] Le Saux S, Aarass H, Lai-Kee-Him J, Bron P, Armengaud J, Miotello G, Bertrand-Michel J, Dubois E, George S, Faklaris O, Devoisselle J-M, Legrand P, Chopineau J, Morille M. Post-production modifications of murine mesenchymal stem cell (mMSC) derived extracellular vesicles (EVs) and impact on their cellular interaction. Biomaterials 2020;231:119675.
- [22] Frank J, Richter M, de Rossi C, Lehr C-M, Fuhrmann K, Fuhrmann G. Extracellular vesicles protect glucuronidase model enzymes during freeze-drying. Sci Rep. 2018:8(1):12377.
- [23] Wu J-Y, Li Y-J, Hu X-B, Huang S, Xiang D-X. Preservation of small extracellular vesicles for functional analysis and therapeutic applications: a comparative evaluation of storage conditions. Drug Deliv 2021;28(1):162–70.

- [24] van de Wakker SI, van Oudheusden J, Mol EA, Roefs MT, Zheng W, Görgens A, et al. Influence of short term storage conditions, concentration methods and excipients on extracellular vesicle recovery and function. Eur J Pharm Biopharm. 2022;170:59–69.
- [25] Herrmann IK, Wood MJA, Fuhrmann G. Extracellular vesicles as a next-generation drug delivery platform. Nat Nanotechnol. 2021;16(7):748–59.
- [26] Born LJ, Chang K-H, Shoureshi P, Lay F, Bengali S, Wei Hsu AT, et al. HOTAIR-loaded mesenchymal stem/stromal cell extracellular vesicles enhance angiogenesis and wound healing. Adv Healthc Mater. 2022;11(5):e2002070.
- [27] Lamichhane TN, Jeyaram A, Patel DB, Parajuli B, Livingston NK, Arumugasaamy N, et al. Oncogene knockdown via active loading of amall RNAs into extracellular vesicles by sonication. Cell Mol Bioeng. 2016;9(3):315–24.
- [28] Pacienza N, Hwa Lee R, Bae E-H, Kim D-K, Liu Q, Prockop DJ, et al. In Vitro macrophage assay predicts the In Vivo anti-inflammatory potential of exosomes from human mesenchymal stromal Cells. Mol Ther Methods Clin Dev. 2019;13:67–76.
- [29] Jeyaram A, Lamichhane TN, Wang S, Zou L, Dahal E, Kronstadt SM, et al. Enhanced loading of functional miRNA cargo via pH gradient modification of extracellular vesicles. Mol Ther. 2020;28(3):975–85.
- [30] Gimona M, Pachler K, Laner-Plamberger S, Schallmoser K, Rohde E. Manufacturing of human extracellular vesicle-based therapeutics for clinical use. Int J Mol Sci. 2017;18(6):1190.
- [31] Maumus M, Rozier P, Boulestreau J, Jorgensen C, Noël D. Mesenchymal stem cell-derived extracellular vesicles: opportunities and challenges for clinical translation. Front Bioeng Biotechnol. 2020;8:997.
- [32] Li Y, Tenchov R, Smoot J, Liu C, Watkins S, Zhou Q. A comprehensive review of the global efforts on COVID-19 vaccine development. ACS Cent Sci. 2021;7(4):512–33.
- [33] Meneghel J, Kilbride P, Shingleton W, Morris J. Ultra-low shipping temperatures for cell therapies. Cytotherapy 2020;22(5):S131. Supplement.
- [34] Bosch S, de Beaurepaire L, Allard M, Mosser M, Heichette C, Chrétien D, et al. Trehalose prevents aggregation of exosomes and cryodamage. Sci Rep. 2016;6:36162.
- [35] Qin B, Zhang Q, Hu X, Mi T, Liu S, Zhang B, et al. How does temperature play a role in the storage of extracellular vesicles? | Cell Physiol. 2020;235(11):7663–80.
- [36] Evtushenko EG, Bagrov DV, Lazarev VN, Livshits MA, Khomyakova E. Adsorption of extracellular vesicles onto the tube walls during storage in solution. PLoS One 2020;15(12):e0243738.